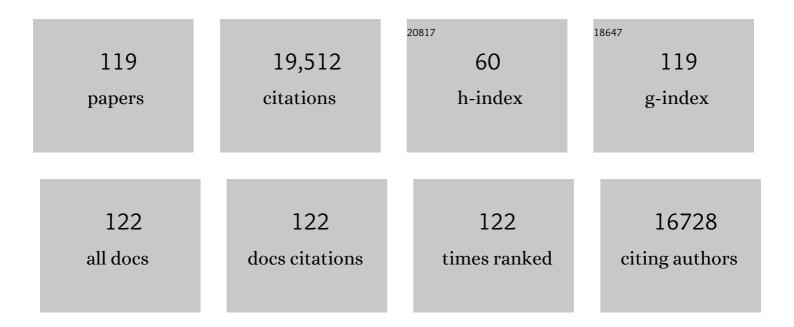
## Francisco Fabregat-Santiago

List of Publications by Year in descending order

Source: https://exaly.com/author-pdf/5985891/publications.pdf Version: 2024-02-01



#	Article	IF	CITATIONS
1	Influence of electrolyte in transport and recombination in dye-sensitized solar cells studied by impedance spectroscopy. Solar Energy Materials and Solar Cells, 2005, 87, 117-131.	6.2	1,107
2	Characterization of nanostructured hybrid and organic solar cells by impedance spectroscopy. Physical Chemistry Chemical Physics, 2011, 13, 9083.	2.8	1,084
3	Characteristics of High Efficiency Dye-Sensitized Solar Cellsâ€. Journal of Physical Chemistry B, 2006, 110, 25210-25221.	2.6	1,015
4	Water Oxidation at Hematite Photoelectrodes: The Role of Surface States. Journal of the American Chemical Society, 2012, 134, 4294-4302.	13.7	895
5	Correlation between Photovoltaic Performance and Impedance Spectroscopy of Dye-Sensitized Solar Cells Based on Ionic Liquids. Journal of Physical Chemistry C, 2007, 111, 6550-6560.	3.1	870
6	General Working Principles of CH <sub>3</sub> NH <sub>3</sub> PbX <sub>3</sub> Perovskite Solar Cells. Nano Letters, 2014, 14, 888-893.	9.1	786
7	Mechanism of carrier accumulation in perovskite thin-absorber solar cells. Nature Communications, 2013, 4, 2242.	12.8	760
8	Recombination in Quantum Dot Sensitized Solar Cells. Accounts of Chemical Research, 2009, 42, 1848-1857.	15.6	747
9	Electron Lifetime in Dye-Sensitized Solar Cells: Theory and Interpretation of Measurements. Journal of Physical Chemistry C, 2009, 113, 17278-17290.	3.1	694
10	Photoelectrochemical and Impedance Spectroscopic Investigation of Water Oxidation with "Co–Pi―Coated Hematite Electrodes. Journal of the American Chemical Society, 2012, 134, 16693-16700.	13.7	635
11	Role of the Selective Contacts in the Performance of Lead Halide Perovskite Solar Cells. Journal of Physical Chemistry Letters, 2014, 5, 680-685.	4.6	583
12	Electrochemical and photoelectrochemical investigation of water oxidation with hematite electrodes. Energy and Environmental Science, 2012, 5, 7626.	30.8	451
13	Electron Transport and Recombination in Solid-State Dye Solar Cell with Spiro-OMeTAD as Hole Conductor. Journal of the American Chemical Society, 2009, 131, 558-562.	13.7	424
14	A perspective on the production of dye-sensitized solar modules. Energy and Environmental Science, 2014, 7, 3952-3981.	30.8	381
15	Cyclic Voltammetry Studies of Nanoporous Semiconductors. Capacitive and Reactive Properties of Nanocrystalline TiO2 Electrodes in Aqueous Electrolyte. Journal of Physical Chemistry B, 2003, 107, 758-768.	2.6	372
16	High Carrier Density and Capacitance in TiO <sub>2</sub> Nanotube Arrays Induced by Electrochemical Doping. Journal of the American Chemical Society, 2008, 130, 11312-11316.	13.7	368
17	Surface Recombination and Collection Efficiency in Perovskite Solar Cells from Impedance Analysis. Journal of Physical Chemistry Letters, 2016, 7, 5105-5113.	4.6	346
18	Doubling Exponent Models for the Analysis of Porous Film Electrodes by Impedance. Relaxation of TiO2Nanoporous in Aqueous Solution. Journal of Physical Chemistry B, 2000, 104, 2287-2298.	2.6	335

#	Article	IF	CITATIONS
19	Understanding the Role of Underlayers and Overlayers in Thin Film Hematite Photoanodes. Advanced Functional Materials, 2014, 24, 7681-7688.	14.9	289
20	Decoupling of Transport, Charge Storage, and Interfacial Charge Transfer in the Nanocrystalline TiO2/Electrolyte System by Impedance Methods. Journal of Physical Chemistry B, 2002, 106, 334-339.	2.6	285
21	Determination of carrier density of ZnO nanowires by electrochemical techniques. Applied Physics Letters, 2006, 89, 203117.	3.3	277
22	A review of recent results on electrochemical determination of the density of electronic states of nanostructured metal-oxide semiconductors and organic hole conductors. Inorganica Chimica Acta, 2008, 361, 684-698.	2.4	276
23	Electron Transport in Dye-Sensitized Solar Cells Based on ZnO Nanotubes: Evidence for Highly Efficient Charge Collection and Exceptionally Rapid Dynamics. Journal of Physical Chemistry A, 2009, 113, 4015-4021.	2.5	255
24	Factors determining the photovoltaic performance of a CdSe quantum dot sensitized solar cell: the role of the linker molecule and of the counter electrode. Nanotechnology, 2008, 19, 424007.	2.6	237
25	Theoretical models for ac impedance of finite diffusion layers exhibiting low frequency dispersion. Journal of Electroanalytical Chemistry, 1999, 475, 152-163.	3.8	228
26	Mott-Schottky Analysis of Nanoporous Semiconductor Electrodes in Dielectric State Deposited on SnO[sub 2](F) Conducting Substrates. Journal of the Electrochemical Society, 2003, 150, E293.	2.9	218
27	Implications of the Negative Capacitance Observed at Forward Bias in Nanocomposite and Polycrystalline Solar Cells. Nano Letters, 2006, 6, 640-650.	9.1	217
28	Analysis of the Origin of Open Circuit Voltage in Dye Solar Cells. Journal of Physical Chemistry Letters, 2012, 3, 1629-1634.	4.6	208
29	Anomalous transport effects in the impedance of porous film electrodes. Electrochemistry Communications, 1999, 1, 429-435.	4.7	195
30	The origin of slow electron recombination processes in dye-sensitized solar cells with alumina barrier coatings. Journal of Applied Physics, 2004, 96, 6903-6907.	2.5	190
31	From Flat to Nanostructured Photovoltaics: Balance between Thickness of the Absorber and Charge Screening in Sensitized Solar Cells. ACS Nano, 2012, 6, 873-880.	14.6	170
32	Carbon Counter-Electrode-Based Quantum-Dot-Sensitized Solar Cells with Certified Efficiency Exceeding 11%. Journal of Physical Chemistry Letters, 2016, 7, 3103-3111.	4.6	169
33	Surface Passivation of Nanoporous TiO <sub>2</sub> via Atomic Layer Deposition of ZrO <sub>2</sub> for Solid-State Dye-Sensitized Solar Cell Applications. Journal of Physical Chemistry C, 2009, 113, 18385-18390.	3.1	141
34	Dye versus Quantum Dots in Sensitized Solar Cells: Participation of Quantum Dot Absorber in the Recombination Process. Journal of Physical Chemistry Letters, 2011, 2, 3032-3035.	4.6	139
35	Water Oxidation at Hematite Photoelectrodes with an Iridium-Based Catalyst. Journal of Physical Chemistry C, 2013, 117, 3826-3833.	3.1	128
36	Energetic factors governing injection, regeneration and recombination in dye solar cells with phthalocyanine sensitizers. Energy and Environmental Science, 2010, 3, 1985.	30.8	125

#	Article	IF	CITATIONS
37	Surface Polarization Model for the Dynamic Hysteresis of Perovskite Solar Cells. Journal of Physical Chemistry Letters, 2017, 8, 915-921.	4.6	122
38	Quantification of the Effects of Recombination and Injection in the Performance of Dye-Sensitized Solar Cells Based on <i>N</i> -Substituted Carbazole Dyes. Journal of Physical Chemistry C, 2010, 114, 19840-19848.	3.1	120
39	Temperature effects in dye-sensitized solar cells. Physical Chemistry Chemical Physics, 2013, 15, 2328.	2.8	111
40	Design and characterization of alkoxy-wrapped push–pull porphyrins for dye-sensitized solar cells. Chemical Communications, 2012, 48, 4368.	4.1	108
41	Identifying charge and mass transfer resistances of an oxygen reducing biocathode. Energy and Environmental Science, 2011, 4, 5035.	30.8	107
42	Diffusion–Recombination Impedance Model for Solar Cells with Disorder and Nonlinear Recombination. ChemElectroChem, 2014, 1, 289-296.	3.4	105
43	Three-Channel Transmission Line Impedance Model for Mesoscopic Oxide Electrodes Functionalized with a Conductive Coating. Journal of Physical Chemistry B, 2006, 110, 11284-11290.	2.6	103
44	Harnessing Infrared Photons for Photoelectrochemical Hydrogen Generation. A PbS Quantum Dot Based "Quasi-Artificial Leaf― Journal of Physical Chemistry Letters, 2013, 4, 141-146.	4.6	101
45	Quantum Dot Based Heterostructures for Unassisted Photoelectrochemical Hydrogen Generation. Advanced Energy Materials, 2013, 3, 176-182.	19.5	101
46	Modelling the electric potential distribution in the dark in nanoporous semiconductor electrodes. Journal of Solid State Electrochemistry, 1999, 3, 337-347.	2.5	99
47	Nature of the Schottky-type barrier of highly dense SnO2 systems displaying nonohmic behavior. Journal of Applied Physics, 2000, 88, 6545-6548.	2.5	99
48	Chemical capacitance of nanoporous-nanocrystalline TiO2in a room temperature ionic liquid. Physical Chemistry Chemical Physics, 2006, 8, 1827-1833.	2.8	99
49	Application of a distributed impedance model in the analysis of conducting polymer films. Electrochemistry Communications, 2000, 2, 601-605.	4.7	98
50	Electronic conductivity in nanostructured TiO2 films permeated with electrolyte. Physica Status Solidi A, 2003, 196, R4-R6.	1.7	97
51	Improved Stability of Inverted and Flexible Perovskite Solar Cells with Carbon Electrode. ACS Applied Energy Materials, 2020, 3, 5126-5134.	5.1	95
52	Exploring Graphene Quantum Dots/TiO2 interface in photoelectrochemical reactions: Solar to fuel conversion. Electrochimica Acta, 2016, 187, 249-255.	5.2	79
53	Origin of efficiency enhancement in Nb2O5 coated titanium dioxide nanorod based dye sensitized solar cells. Energy and Environmental Science, 2011, 4, 3414.	30.8	75
54	Impedance Spectroscopy Analysis of the Effect of TiO <sub>2</sub> Blocking Layers on the Efficiency of Dye Sensitized Solar Cells. Journal of Physical Chemistry C, 2012, 116, 12415-12421.	3.1	73

#	Article	IF	CITATIONS
55	Effect of Energy Disorder in Interfacial Kinetics of Dye-Sensitized Solar Cells with Organic Hole Transport Material. Journal of Physical Chemistry B, 2006, 110, 19406-19411.	2.6	71
56	Interpretation of Cyclic Voltammetry Measurements of Thin Semiconductor Films for Solar Fuel Applications. Journal of Physical Chemistry Letters, 2013, 4, 1334-1339.	4.6	69
57	Impedance spectroscopy of thin-film CdTe/CdS solar cells under varied illumination. Journal of Applied Physics, 2009, 106, .	2.5	68
58	Enhanced Carrier Transport Distance in Colloidal PbS Quantum-Dot-Based Solar Cells Using ZnO Nanowires. Journal of Physical Chemistry C, 2015, 119, 27265-27274.	3.1	65
59	Deleterious Effect of Negative Capacitance on the Performance of Halide Perovskite Solar Cells. ACS Energy Letters, 2017, 2, 2007-2013.	17.4	65
60	Negative Capacitance and Inverted Hysteresis: Matching Features in Perovskite Solar Cells. Journal of Physical Chemistry Letters, 2020, 11, 8417-8423.	4.6	63
61	Determination of electron and hole energy levels in mesoporous nanocrystalline TiO2 solid-state dye solar cell. Synthetic Metals, 2006, 156, 944-948.	3.9	62
62	Overcoming Charge Collection Limitation at Solid/Liquid Interface by a Controllable Crystal Deficient Overlayer. Advanced Energy Materials, 2017, 7, 1600923.	19.5	61
63	Impedance spectroscopy study of dye-sensitized solar cells with undoped spiro-OMeTAD as hole conductor. Journal of Applied Physics, 2006, 100, 034510.	2.5	59
64	Elucidating Capacitance and Resistance Terms in Confined Electroactive Molecular Layers. Analytical Chemistry, 2013, 85, 411-417.	6.5	58
65	Electron injection and scaffold effects in perovskite solar cells. Journal of Materials Chemistry C, 2017, 5, 634-644.	5.5	58
66	Near-IR sensitization of wide band gap oxide semiconductor by axially anchored Si-naphthalocyanines. Energy and Environmental Science, 2009, 2, 529.	30.8	57
67	Selective contacts drive charge extraction in quantum dot solids via asymmetry in carrier transfer kinetics. Nature Communications, 2013, 4, 2272.	12.8	56
68	Chemical Effects of Tin Oxide Nanoparticles in Polymer Electrolytes-Based Dye-Sensitized Solar Cells. Journal of Physical Chemistry C, 2014, 118, 16510-16517.	3.1	56
69	Competitive Photoelectrochemical Methanol and Water Oxidation with Hematite Electrodes. ACS Applied Materials & Interfaces, 2015, 7, 7653-7660.	8.0	56
70	Carrier density and interfacial kinetics of mesoporous TiO2 in aqueous electrolyte determined by impedance spectroscopy. Journal of Electroanalytical Chemistry, 2012, 668, 119-125.	3.8	54
71	Hydrazine sensors development based on a glassy carbon electrode modified with a nanostructured TiO2 films by electrochemical approach. Mikrochimica Acta, 2017, 184, 2123-2129.	5.0	53
72	Quantification of bio-anode capacitance in bioelectrochemical systems using Electrochemical Impedance Spectroscopy. Journal of Power Sources, 2018, 400, 533-538.	7.8	50

#	Article	IF	CITATIONS
73	Three dimensional-TiO2 nanotube array photoanode architectures assembled on a thin hollow nanofibrous backbone and their performance in quantum dot-sensitized solar cells. Chemical Communications, 2013, 49, 2810.	4.1	48
74	Dynamic Processes in the Coloration of WO[sub 3] by Lithium Insertion. Journal of the Electrochemical Society, 2001, 148, E302.	2.9	45
75	Modeling and characterization of extremely thin absorber (eta) solar cells based on ZnO nanowires. Physical Chemistry Chemical Physics, 2011, 13, 7162.	2.8	45
76	Analysis of bio-anode performance through electrochemical impedance spectroscopy. Bioelectrochemistry, 2015, 106, 64-72.	4.6	45
77	Switching behaviour in lightly doped polymeric porous film electrodes. Improving distributed impedance models for mixed conduction conditions. Journal of Electroanalytical Chemistry, 2001, 508, 48-58.	3.8	43
78	Hole conductivity and acceptor density of p-type CuGaO2 nanoparticles determined by impedance spectroscopy: The effect of Mg doping. Electrochimica Acta, 2013, 113, 570-574.	5.2	43
79	SiO2 Aerogel Templated, Porous TiO2 Photoanodes for Enhanced Performance in Dye-Sensitized Solar Cells Containing a Ni(III)/(IV) Bis(dicarbollide) Shuttle. Journal of Physical Chemistry C, 2011, 115, 11257-11264.	3.1	38
80	Joint Photophysical and Electrical Analyses on the Influence of Conjugation Order in D-ï€-A Photosensitizers of Mesoscopic Titania Solar Cells. Journal of Physical Chemistry C, 2011, 115, 14425-14430.	3.1	37
81	Doping saturation in dye-sensitized solar cells based on ZnO:Ga nanostructured photoanodes. Electrochimica Acta, 2011, 56, 6503-6509.	5.2	36
82	Bandgap Modulation in Efficient <i>n</i> â€Thiophene Absorbers for Dye Solar Cell Sensitization. ChemPhysChem, 2010, 11, 245-250.	2.1	35
83	The combination of a polymer–carbon composite electrode with a high-absorptivity ruthenium dye achieves an efficient dye-sensitized solar cell based on a thiolate–disulfide redox couple. Physical Chemistry Chemical Physics, 2012, 14, 7131.	2.8	35
84	Relaxation processes in the coloration of amorphous WO3 thin films studied by combined impedance and electro-optical measurements. Journal of Applied Physics, 2004, 96, 853-859.	2.5	34
85	Effect of trap density on the dielectric response of varistor ceramics. Solid-State Electronics, 1999, 43, 2123-2127.	1.4	32
86	Interfacial engineering of quantum dot-sensitized TiO2 fibrous electrodes for futuristic photoanodes in photovoltaic applications. Journal of Materials Chemistry, 2012, 22, 14228.	6.7	32
87	In situ Biofilm Quantification in Bioelectrochemical Systems by using Optical Coherence Tomography. ChemSusChem, 2018, 11, 2171-2178.	6.8	30
88	Electron trapping induced electrostatic adsorption of cations: a general factor leading to photoactivity decay of nanostructured TiO <sub>2</sub> . Journal of Materials Chemistry A, 2017, 5, 6455-6464.	10.3	29
89	Stability of dye-sensitized solar cells under extended thermal stress. Physical Chemistry Chemical Physics, 2017, 19, 22546-22554.	2.8	28
90	Panchromatic Solar-to-H <sub>2</sub> Conversion by a Hybrid Quantum Dots–Dye Dual Absorber Tandem Device. Journal of Physical Chemistry C, 2014, 118, 891-895.	3.1	27

#	Article	IF	CITATIONS
91	Analysis of cyclic voltammograms of electrochromic a-WO3 films from voltage-dependent equilibrium capacitance measurements. Journal of Electroanalytical Chemistry, 2004, 565, 329-334.	3.8	26
92	Anomalous transport on polymeric porous film electrodes in the dopant-induced insulator-to-conductor transition analyzed by electrochemical impedance. Applied Physics Letters, 2001, 78, 1885-1887.	3.3	25
93	Dynamic behaviour of viologen-activated nanostructured TiO2: correlation between kinetics of charging and coloration. Electrochimica Acta, 2004, 49, 745-752.	5.2	25
94	TiO <sub>2</sub> Nanotubes for Solar Water Splitting: Vacuum Annealing and Zr Doping Enhance Water Oxidation Kinetics. ACS Omega, 2019, 4, 16095-16102.	3.5	24
95	Enhanced diffusion through porous nanoparticle optical multilayers. Journal of Materials Chemistry, 2012, 22, 1751-1757.	6.7	22
96	Combining Modulated Techniques for the Analysis of Photosensitive Devices. Small Methods, 2021, 5, e2100661.	8.6	22
97	Charging and diffusional aspects of Li+ insertion in electrochromic a-WO3. Solid State Ionics, 2004, 175, 521-525.	2.7	21
98	Injection and Recombination in Dye-Sensitized Solar Cells with a Broadband Absorbance Metal-Free Sensitizer Based on Oligothienylvinylene. Journal of Physical Chemistry C, 2008, 112, 18623-18627.	3.1	20
99	Effect of Environmental Humidity on the Electrical Properties of Lead Halide Perovskites. Journal of Physical Chemistry C, 2019, 123, 2011-2018.	3.1	20
100	Tuning the selectivity of biomass oxidation over oxygen evolution on NiO–OH electrodes. Green Chemistry, 2021, 23, 8061-8068.	9.0	20
101	Revealing the contribution of singlet oxygen in the photoelectrochemical oxidation of benzyl alcohol. Sustainable Energy and Fuels, 2021, 5, 956-962.	4.9	18
102	Role of Pd in the Electrochemical Hydrogenation of Nitrobenzene Using CuPd Electrodes. Advanced Sustainable Systems, 2022, 6, .	5.3	16
103	Grain boundary role in the electrical properties of La1â^'xSrxCo0.8Fe0.2O3â^´î´ perovskites. Solid State Ionics, 1998, 107, 203-211.	2.7	14
104	Frequency dispersion in electrochromic devices and conducting polymer electrodes: A generalized transmission line approach. Ionics, 1999, 5, 44-51.	2.4	14
105	Electron-Transfer Kinetics through Interfaces between Electron-Transport and Ion-Transport Layers in Solid-State Dye-Sensitized Solar Cells Utilizing Solid Polymer Electrolyte. Journal of Physical Chemistry C, 2016, 120, 2494-2500.	3.1	13
106	Determination of the humidity of soil by monitoring the conductivity with indium tin oxide glass electrodes. Applied Physics Letters, 2002, 80, 2785-2787.	3.3	10
107	Impedance spectroscopic analysis of high-performance dye sensitized solar cells based on nano-clay electrolytes. Electrochimica Acta, 2016, 197, 77-83.	5.2	8
108	Structural and electrical conductivity studies on rutile solid solutions [FexTi1-2xMxO2 (M=Nb, Ta)]. Journal of Materials Science, 1998, 33, 4235-4238.	3.7	7

#	Article	IF	CITATIONS
109	EFFECT OF THE CHROMOPHORES STRUCTURES ON THE PERFORMANCE OF SOLID-STATE DYE SENSITIZED SOLAR CELLS. Nano, 2014, 09, 1440005.	1.0	7
110	Pencil graphite rods decorated with nickel and nickel–iron as low-cost oxygen evolution reaction electrodes. Sustainable Energy and Fuels, 2021, 5, 3929-3938.	4.9	7
111	C <sub>60</sub> Thin Films in Perovskite Solar Cells: Efficient or Limiting Charge Transport Layer?. ACS Applied Energy Materials, 2022, 5, 1646-1655.	5.1	6
112	Experimental Characterization and Statistical Analysis of Waterâ€Based Gold Nanofluids for Solar Applications: Optical Properties and Photothermal Conversion Efficiency. Solar Rrl, 2022, 6, .	5.8	6
113	Direct Observation of the Chemical Transformations in BiVO <sub>4</sub> Photoanodes upon Prolonged Lightâ€Aging Treatments. Solar Rrl, 2022, 6, .	5.8	5
114	The role of instrumentation in the process of modeling real capacitors. IEEE Transactions on Education, 2000, 43, 439-442.	2.4	4
115	Platinum-coated nanostructured oxides for active catalytic electrodes. Catalysis Communications, 2011, 14, 58-61.	3.3	4
116	Impedance Spectroscopy in Molecular Devices. Green Chemistry and Sustainable Technology, 2018, , 353-384.	0.7	4
117	Co-adsorbing effect of bile acids containing bulky amide groups at 3β-position on the photovoltaic performance in dye-sensitized solar cells. Solar Energy, 2019, 189, 94-102.	6.1	4
118	Impedance spectroscopy study of solid-state dye-sensitized solar cells with varying Spiro-OMeTAD concentration. Materials Research Society Symposia Proceedings, 2009, 1211, 1.	0.1	0
119	Influence of alumina coating on transport and recombination in DSSCs with 1-methylbenzidazole as electrolyte additives. Proceedings of SPIE, 2009, , .	0.8	0